Semicond. Sci. Technol. **27** (2012) 105013 (6pp) doi:10.1088/0268-1242/27/10/105013

Effects of a key deep level and interface states on the performance of GaAsN solar cells: a simulation analysis

Xiuxun Han[1,2], Jong-Ha Hwang[3], Nobuaki Kojima[3], Yoshio Ohshita[3] and Masafumi Yamaguchi[3]

[1] Laboratory of Clean Energy Chemistry and Materials, Lanzhou Institute of Chemical Physics, Chinese Academy of Sciences, Lanzhou 730000, People's Republic of China
[2] State Key Laboratory of Solid Lubrication, Lanzhou Institute of Chemical Physics, Chinese Academy of Sciences, Lanzhou 730000, People's Republic of China
[3] Toyota Technological Institute, 2-12-1 Hisakata, Tempaku, Nagoya 468-8511, Japan

E-mail: xxhan@licp.cas.cn

Received 12 April 2012, in final form 21 June 2012
Published 6 August 2012
Online at stacks.iop.org/SST/27/105013

Abstract
To explore the origin of low conversion efficiency of GaAsN solar cells, the effects from a key deep level (E1) at about 0.3–0.4 eV below the conduction band and interface states between the GaAsN emitter and GaAs front surface field layer were investigated by numerical simulation. Our results show that a high deep level concentration in GaAsN layers and a large interface recombination velocity are necessary to fit the experimental data. Interface recombination plays an important role in reducing the quantum efficiency in the short-wavelength region. Its effect can be weakened by applying a thin emitter and a high doping level in the GaAs surface field layer. The abundant existence of E1 is responsible for the high contribution of Shockley–Read–Hall recombination from the space-charged region. Its density should be reduced to $<10^{15}$ cm^{-3} for higher conversion efficiency.

(Some figures may appear in colour only in the online journal)

1. Introduction

The electrical and optical properties of Ga (In) AsN materials degrade dramatically with the incorporation of N, which limit the conversion efficiency of Ga(In)AsN-based solar cell device to a relatively low level [1, 2]. Clarifying the manners in which the key crystal parameters influence the device performance is believed to facilitate further improvements. Experimental efforts and theoretical simulations are complementary in approaching such a goal [3]. An important *N*-related deep level (E1) 0.2–0.3 eV below the conduction band has already been identified to deteriorate the open circuit voltage V_{oc} significantly via the deep level transient spectroscopy (DLTS) method [1, 4–6]. It is further revealed that this electron trap is up to 0.1 eV deeper than the measured activation energies due to the Poole–Frenkel effect [7]. Although the exact structure of E1 is unknown so far, possible candidates include $(N\text{-}N)_{As}$ and $(N\text{-}As)_{As}$ [8, 9]. The large electron capture cross section of 10^{-15}–10^{-14} cm^2 indicates that this defect might be an efficient non-radiative recombination center [4, 9]. Theoretical calculations also predict a low formation energy for $(N\text{-}N)_{As}$ split interstitials [10]. On the other hand, an interface recombination velocity (S) higher than 10^4 cm s^{-1} was detected by the time-resolved photoluminescence method in nominally undoped GaAs/GaAsN heterojunctions [11], which might affect the efficient collection of photogenerated carriers because GaAs is usually utilized as the surface field (SF) layer in GaAsN-based solar cells [12, 13]. How and to what extent those two important material factors impact the device performance has not been fully studied yet. In an attempt to provide an appropriate evaluation on GaAsN solar cell performance, we first fit the experimental data to get the reliable defect parameters for both the key defect E1 and the front GaAs/GaAsN interface recombination. Then numerical simulations were performed to clarify their influences on main device factors. Possible ways to weaken their effects were discussed.

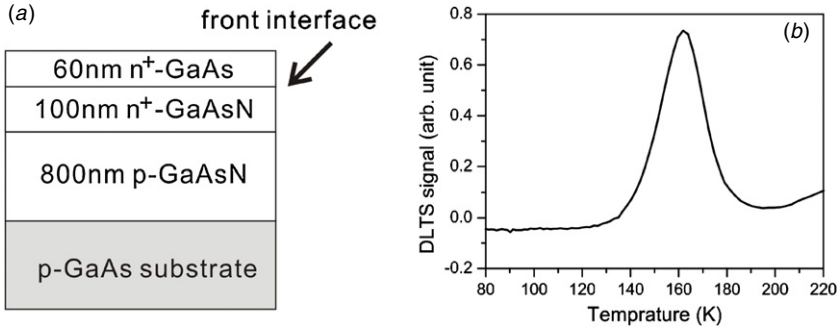

Figure 1. (*a*) The GaAsN solar cell structure and (*b*) the typical DLTS spectrum for a separate Si-doped GaAsN sample. The peak in (*b*) corresponds to the E1 defect.

Table 1. Device parameters for an n^+–p GaAsN homojunction solar cell grown by CBE.

Layer properties	p-GaAsN	n^+-GaAsN	n^+-GaAs
Thickness (μm)	0.8	0.1	0.06
Bandgap (eV)	1.28	1.28	1.42
Doping level (cm^{-3})	1×10^{16}	3×10^{17}	2×10^{18}
Electron mobility ($cm^2\ V^{-1}\ s^{-1}$)	300	300	8500
Hole mobility ($cm^2\ V^{-1}\ s^{-1}$)	100	100	400

2. Device structure and simulation methods

The data used during the simulation are based on the experimental results of an n^+–p GaAsN homojunction solar cell grown by a chemical beam epitaxy (CBE) system. Along the light incident direction, the device consists of a heavily Si-doped GaAs SF layer, a Si-doped GaAsN emitter, an unintentionally doped p-GaAsN base layer and a heavily doped p-GaAs substrate (see figure 1(*a*)). The N composition in the GaAsN active layer was measured to be 0.73%, which corresponds to a bandgap of about 1.28 eV. Main device parameters are listed in table 1.

The simulation was performed via computer software SCAPS developed by University of Gent [14]. It numerically solves the Poisson equation and the electron and hole continuity equations in one dimension. In each layer, up to three deep levels can be defined in addition to the shallow dopants. Here, we introduced an acceptor-like defect in both n- and p-type GaAsN layers in addition to E1. Its existence has been confirmed by DLTS studies [15]. It is located at ~0.15 eV above the valence band edge with a typical density of $\sim 5 \times 10^{15}$ cm^{-3}. A capture cross section ratio of 100 for holes and electrons was assigned, which renders it to behave as a hole trap rather than an effective recombination center and accounts for the usually observed p-type background doping in unintentionally doped GaAsN [15]. Figure 1(*b*) illustrates the typical DLTS spectrum for a separate Si-doped GaAsN sample under the growth condition comparable to the active layer of the solar cell. The existence of E1 defect was confirmed in our GaAsN layer. Since the exact hole capture cross section has not been reported yet, the measured electron capture cross section of 8.9×10^{-15} cm^2 was also assigned to the hole to account for the recombination nature of E1 [4]. The Schockley–Read–Hall (SRH) formalism is used to describe the recombination and occupation behavior of those defect levels in SCAPS. For recombination via the interface states, SCAPS allows the exchange of electrons (holes) between interface states and two adjacent conduction (valence) bands by following an extended SRH formalism [14]. In this work, only interface states between the n-GaAsN emitter and the n-GaAs SF layer are discussed because our calculation results revealed that effects on the cell performance from the absorber/substrate interface states were minimal under the typical simulation condition. This is mainly due to the high absorbance and relatively short minority carrier lifetime in GaAsN layers. Since no convincing information on the location and electronic structure of GaAs/GaAsN interface states is available yet, the front interface states are assumed to be distributed uniformly over the midgap of GaAsN with a characteristic energy of 0.5 eV. Furthermore, the interface states are of neutral character and do not influence the band diagram. Such a treatment sets a direct correlation between the defect density and the nominal interface recombination velocity, while the latter can be evaluated from experiments [11]. To fit the experimental data, all experimentally available device parameters in table 1 were utilized. For convenience, the absorption coefficient was obtained by a linear shift of the GaAs absorption spectrum to the GaAsN absorption edge. This might cause a slight deviation at the low-energy side of the absorption edge due to the GaAsN band tail caused by composition inhomogeneity, but will not influence the discussions on the front interface and bulk defects significantly. The electron and hole mobilities were set to 300 and 100 $cm^2\ V^{-1}\ s^{-1}$, respectively, our typical values for single GaAsN layers grown under the similar conditions. Finally, area-normalized series/shunt resistance, interface recombination velocity, surface reflection, the density (Nt) and energy depth of E1 are left as adjustable parameters to fit the experimental *J–V* curves and external quantum efficiency (EQE).

3. Results and discussion

3.1. Fitting to the experimental data

Fitting results to the measured dark *J–V* curve, illuminated *J–V* curve, and EQE of a GaAsN homojunction solar cell grown by CBE system are shown in figures 2(*a*), (*b*) and (*c*), respectively. An external series resistance of $R_s = 3.5\ \Omega\ cm^2$ and a finite

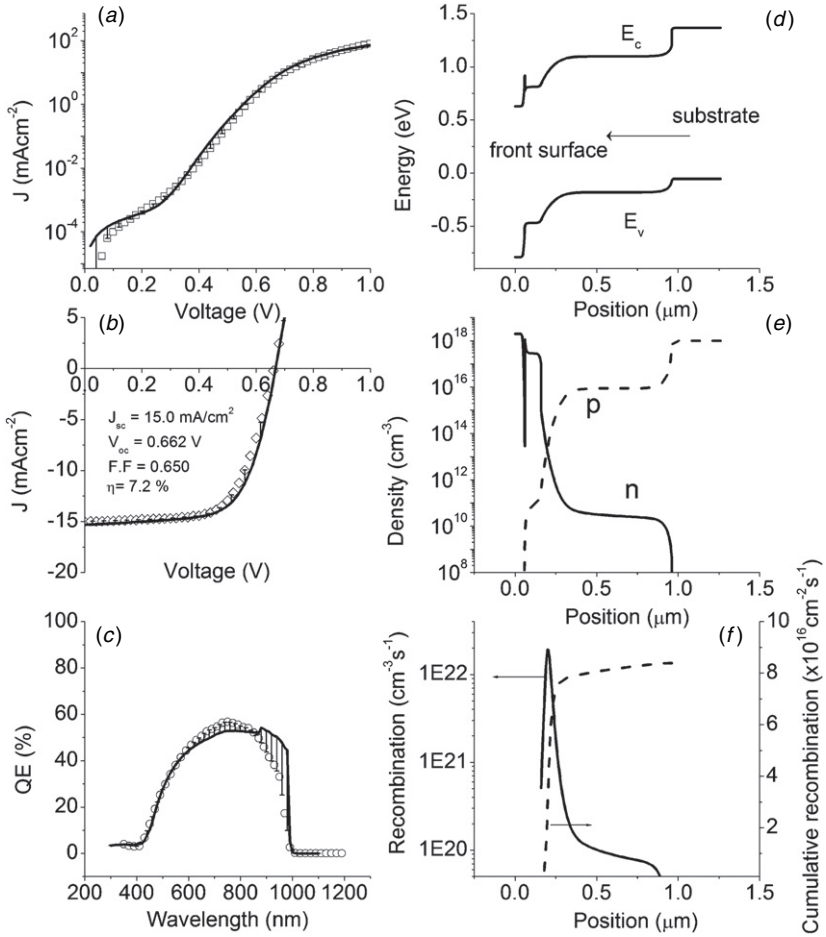

Figure 2. Measured data (symbols) and simulated results by SCAPS (lines) for (*a*) dark *J*–*V* curves, (*b*) illuminated *J*–*V* curve and (*c*) external quantum efficiency. Error bars are given to show the deviations of the simulated curves from the experimental data. The simulations for (*d*) band energy, (*e*) carrier density and (*f*) bulk recombination rate were performed in dark under the electric forward bias that corresponds to the V_{oc} of the same device under illumination.

shunt resistance of $R_{sh} = 5.5 \times 10^5\ \Omega\ cm^2$ were introduced to be responsible for the dark *J*–*V* characteristics in the high- and low-voltage ranges, respectively. Since the capture cross sections of E1 were fixed to the measured values, the slope of the linear part of the dark *J*–*V* curve, which is deviated from q/kT, is mainly dependent on the energy depth of E1. Nt can be determined from the magnitude of dark current in this voltage range on one side, and also accounts for the EQE in the middle-wavelength region on the other. Front interface recombination is the key limiting factor for the EQE at short wavelengths. The surface reflection was adjusted to complete the fitting to both light *J*–*V* curve and EQE. Satisfactory agreements can be achieved as the parameters in table 2 were applied. The fitting procedure revealed the reasonable excitation energy of ∼0.38 eV for E1, which lies in the practical energy region predicted by DLTS [7]. Furthermore, Nt was evaluated to be $8 \times 10^{15}\ cm^{-3}$. The interface recombination velocity is as high as $4.3 \times 10^5\ cm\ s^{-1}$, which is expected to affect the collection of a photo-generated carrier in the emitter significantly. In figure 2(*f*), the bulk recombination rate in the dark is plotted as a function of position to reveal the dominant recombination regime under the fitting condition. The device was simulated under a forward bias matching to the V_{oc} of the same cell structure under illumination. The corresponding band energy and carrier density are illustrated in figures 2(*d*) and (*e*). As can be seen, the recombination rate has a maximum in the space-charged region. In contrast, it is very weak in the quasi-neutral region. The cumulative recombination rate further confirms

Table 2. Parameters used during fitting experimental results.

Adjustable fitting parameters	Value
Area normalized series resistance (Ω cm^2)	3.5
Area normalized shunt resistance (× 10^5 Ω cm^2)	5.5
Surface reflection	0.29
Density of deep level E1 (cm^3)	8 × 10^{15}
Excitation energy of E1 (eV)	0.38
Front interface recombination velocity (cm s^{-1})	4.3 × 10^5
Fixed fitting parameters	
Capture cross section of E1 (electron, × 10^{-15} cm^2)[a]	8.9
Capture cross section of E1 (hole, × 10^{-15} cm^2)	8.9
Capture cross section of H1 (electron, × 10^{-18} cm^2)	1
Capture cross section of H1 (hole, × 10^{-16} cm^2)[b]	1
Concentration of H1 (× 10^{15} cm^{-3})[b]	5

[a] [4].
[b] [15].

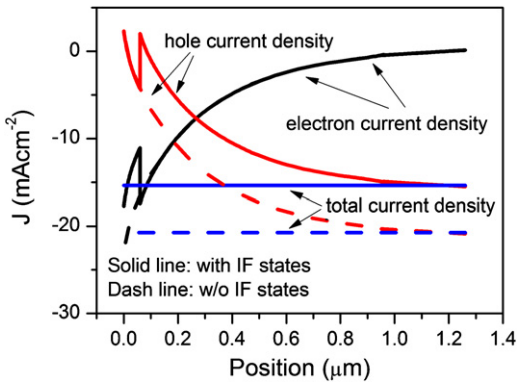

Figure 3. The calculated electron current density component, hole current density component and total current density at short circuit for structures with (solid line) and without (dash line) front interface states.

that the position of n≈p and its surroundings account for the main recombination for such a high deep level density.

To clarify the effects of front interface recombination on the short circuit current density J_{sc}, the electron and hole current density components at short circuit are presented in figure 3. The simulated results for the cell without interface states are also given as the dashed lines for a parallel comparison. For the case without interface states, both electrons and holes carry J_{sc} except for the narrow region close to the front surface. At the front surface, the high surface recombination at the level of 5×10^6 cm s^{-1} leads to the recombination sink for holes. The majority of electrons start to compensate for the hole's positive motion opposite to the direction of photocurrent. After the introduction of interface states, however, the unhelpful behavior of holes can be seen not only at the front, but also in the region close to the GaAs/GaAsN interface (0.06 μm to the surface). This is arising because the hole diffuses to the interface recombination sink due to the large S_p. As a result, J_{sc} remarkably decreases from ∼21 mA cm^{-2} to ∼15 mA cm^{-2} for the cell with the introduction of abundant GaAs/GaAsN interface states.

3.2. Effects of deep level E1

For absorbers with short carrier lifetime, widening the depletion region is commonly utilized to enhance the photo-generated carrier collection via, e.g., further reducing the doping level in GaAsN base layer relative to the emitter. Based on the basic defect parameters deduced from the fitting results, we can examine the correlation between the base doping level and cell performance within a reasonable density region of E1. Figure 4 shows the calculated J_{sc}, V_{oc}, and the conversion efficiency η as a function of Nt with three different doping levels in the base layer. Note that to focus our attentions on the key factors, the surface reflection was set to an ideal value of 10%, and the influences from R_s and R_{sh} were neglected during the calculation. As can be seen, dramatic degradation occurs in both J_{sc} and V_{oc} as the density of E1 exceeds respective critical values (Ntc), which depend on the doping level. For defect density larger than Ntc, J_{sc} linearly decreases with Nt while keeping the same slope for various

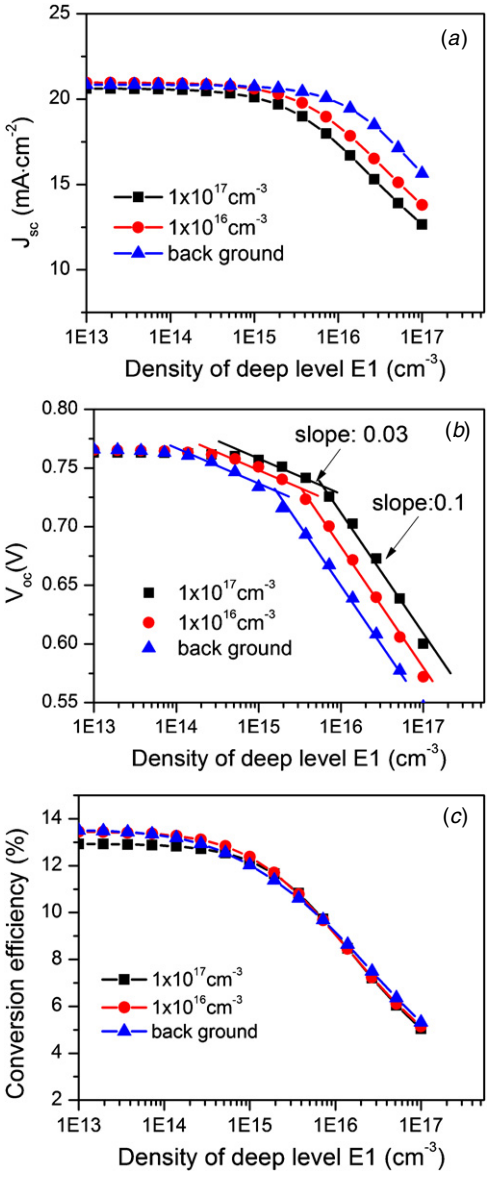

Figure 4. Calculated (*a*) J_{sc}, (*b*) V_{oc} and (*c*) conversion efficiency as a function of E1 density at different doping levels in the p-GaAsN base layer. The surface reflection was set to 10%, and R_s/R_{sh} was neglected during the calculation.

doping levels. The slope depends only on the illumination conditions and the material absorption as predicted by an analytical approach [16]. In contrast, two distinct regimes can be distinguished for V_{oc} in the degradation region. The slope of ∼0.03 is the character of the diffusion-dominant regime with the analytical form of 2.3 kT/2q, while the recombination-dominant regime is characterized by a steep slope of ∼0.1. The slope for the recombination-dominant regime is determined by the location of E1 relative to the intrinsic Fermi level, and has the analytical form of 2.3 nkT/q, where n is the ideal factor of the junction [16]. The influence of the doping level in the base layer on J_{sc} and V_{oc} is remarkable just as Nt > Ntc. As expected, efficient drift collection of the photo-generated carrier leads to an increasing J_{sc} at the low doping level in the base layer. Unfortunately, this merit is balanced out by

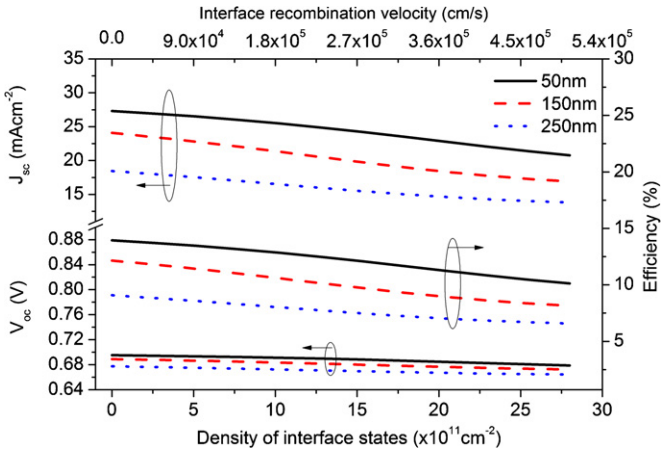

Figure 5. Influence of the interface recombination velocity on the performance of solar cells with different emitter thicknesses (surface reflection: 10%; E1 density: 8×10^{15} cm^{-3}; R_s/R_{sh}: neglected).

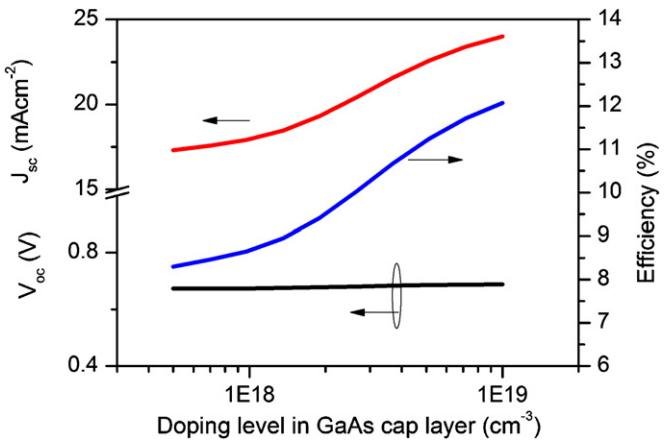

Figure 6. Influence of the doping level in the GaAs cap layer on the solar cell performance (emitter thickness: 100 nm; doping in emitter: 3×10^{17} cm^{-3}; surface reflection: 10%; E1 density: 8×10^{15} cm^{-3}; S_p: 4.3×10^5 cm s^{-1}; R_s/R_{sh}: neglected).

the simultaneous degradation in V_{oc} due to reducing p-type doping. The combined effect is that minor changes can be found in the final conversion efficiency if the doping level is the only adjustable parameter for Nt > Ntc. Simulation results also reveal that E1 density needs to be reduced at least to enter the diffusion-limited regime for realizing a relatively high efficiency.

3.3. Effects of interface recombination

The potential barrier between the GaAs window layer and the GaAsN emitter is powerful to block the diffusion of minority holes toward the front surface. However, the unwanted high interface recombination at the front GaAs/GaAsN interface forms a sink for holes generated in the emitter. The simulation results involving the width of the emitter and interface state density are given in figure 5. Although the most effective way is obviously to reduce the interface states, further experimental efforts are needed to reveal the details on their generations so far. To weaken the effect from front interface recombination, we need a short emitter to guarantee a large portion of absorption occurring in the absorber rather than the emitter. According to the band alignment close to the front interface, interface states mainly communicate with the conduction and valance bands of the GaAsN emitter. The electron concentration at the interface is much higher than the hole concentration in the emitter. Thus, the interface defects are largely occupied by electrons, the majority carrier at the interface. Interface recombination is governed by the availability of free holes near the emitter surfaces. Accordingly, the window/emitter doping ratio also has a strong impact on the interface recombination through changing the potential barrier for holes. Figure 6 presents the simulated cell performance as a function of doping level in the GaAs window layer with the electron concentration in the GaAsN emitter fixed to 3×10^{17} cm^{-3}. The conversion efficiency can be improved to ~12% as the doping level in the window layer increases to 1×10^{19} cm^{-3}, which mainly benefits from the increasing J_{sc}. Both methods to weaken front interface recombination have minor influences on the V_{oc} as could be anticipated. If progress in the GaAsN epitaxial process could be realized, e.g., with E1 density reduced to a level of 10^{14} cm^{-3}, and the interface recombination velocity suppressed to 5×10^4 cm s^{-1}, our simulation shows that a high efficiency of ~20% can be expected.

4. Conclusions

The numerical simulation was performed on a GaAsN homojunction solar cell. A high density of deep defects E1 ~0.3–0.4 eV below the conduction band edge and a high recombination velocity at the front GaAs/GaAsN interface are found to be important efficiency-limiting factors by fitting to the experimental data. To approach higher conversion efficiency, E1 density needs to be reduced to enter the diffusion dominant regime. Furthermore, a relatively thin emitter and a proper doping ratio between the GaAs front surface field layer and the GaAsN emitter should be applied to reduce the effects from the front GaAs/GaAsN interface recombination.

Acknowledgments

Part of this work is supported by the 'Top Hundred Talents Program' of Chinese Academy of Sciences and the New Energy Development Organization (NEDO) under the ministry of Economy, Trade and Industry, Japan

References

[1] Kurtz S, Johnston S and Branz H M 2005 *Appl. Phys. Lett.* **86** 113506
[2] Friedman D J and Kurtz S R 2002 *Prog. Photovolt., Res. Appl.* **10** 331
[3] Igalson M, Zabierowski P, Przado D, Urbaniak A, Edoff M and Shafarman W N 2009 *Sol. Energy Mater. Sol. Cells* **93** 1290
[4] Khan A, Kurtz S R, Prasad S, Johnston S W and Gou J 2007 *Appl. Phys. Lett.* **90** 243509

[5] Krispin P, Spruytte S G, Harris J S and Ploog K H 2002 *Appl. Phys. Lett.* **80** 2120
[6] Johnston S W, Kurtz S R, Friedman D J, Ptak A J, Ahrenkiel R K and Crandall R S 2005 *Appl. Phys. Lett.* **86** 072109
[7] Johnston S W and Kurtz S R 2006 *J. Vac. Sci. Technol.* A **24** 1252
[8] Luther J M, Johnston S W, Kurtz S R, Ahrenkiel R K and Collins R T 2006 *Appl. Phys. Lett.* **88** 263502
[9] Krispin P, Gambin V, Harris J S and Ploog K H 2003 *J. Appl. Phys.* **93** 6095
[10] Zhang S B and Wei S 2001 *Phys. Rev. Lett.* **86** 1789
[11] Honda T, Ikeda K, Inagaki M, Suzuki H, Kojima N, Ohshita Y and Yamaguchi M 2011 *Japan. J. Appl. Phys.* **50** 08KD06
[12] Dimroth F, Baur C, Bett A W, Volz K and Stolz W 2004 *J. Cryst. Growth* **272** 726
[13] Ptak A J, France R, Jiang C S and Romero M J 2009 *J. Cryst. Growth* **311** 1876
[14] Burgelman M, Nollet P and Degrave S 2000 *Thin Solid Films* **361–362** 527
[15] Bouzazi B, Suzuki H, Kojima N, Ohshita Y and Yamaguchi M 2010 *Japan. J. Appl. Phys.* **49** 121001
[16] Bourgoin J C and Zazoui M 2002 *Semicond. Sci. Technol.* **17** 453